Nationaal Lucht- en Ruimtevaartlaboratorium

National Aerospace Laboratory NLR

NLR-TP-2014-528

Aerodynamic design of engine intake duct shape of a general aviation turboprop aircraft

B.I. Soemarwoto, O.J. Boelens and A. Kanakis

Nationaal Lucht- en Ruimtevaartlaboratorium
National Aerospace Laboratory NLR

Anthony Fokkerweg 2
P.O. Box 90502
1006 BM Amsterdam
The Netherlands
Telephone +31 (0)88 511 31 13
Fax +31 (0)88 511 32 10
www.nlr.nl

Nationaal Lucht- en Ruimtevaartlaboratorium
National Aerospace Laboratory NLR

Executive summary

Aerodynamic design of engine intake duct shape of a general aviation turboprop aircraft

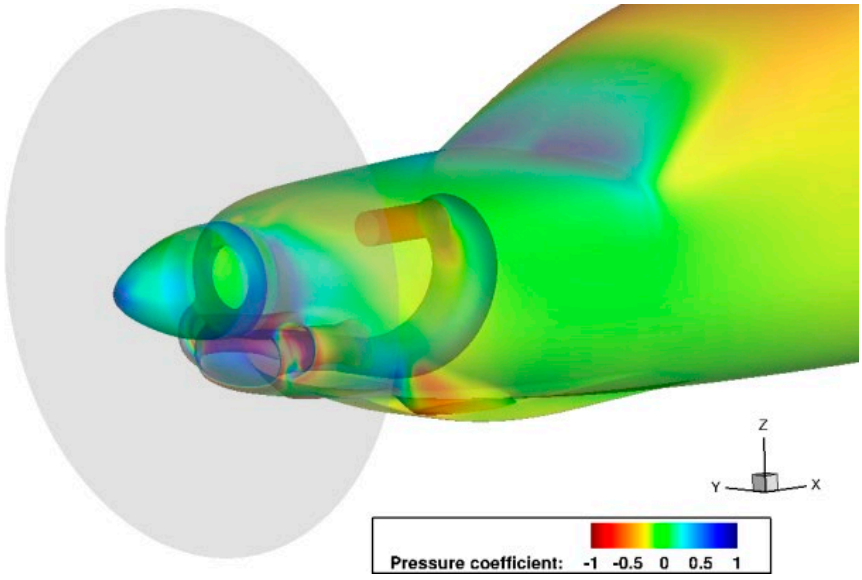

Report no.
NLR-TP-2014-528

Author(s)
B.I. Soemarwoto
O.J. Boelens
A. Kanakis

Report classification
UNCLASSIFIED

Date
July 2016

Knowledge area(s)
Computational Physics en theoretische aërodynamica
Gasturbinetechnologie

Descriptor(s)
CFD design
Adjoint method
Gas turbine
Inver design

Problem area
The aerodynamic design of an engine intake duct shape is described. The design is aimed at obtaining desirable air characteristics into the compressor of a single-engine general aviation turboprop aircraft. The desirable characteristics are based on certain requirements that need to be satisfied for an acceptable quality of the delivered air at a given target mass flow. This has to be achieved subject to structural constraints requiring that the shape modification must respect the internal contents of the engine nacelle, such as the firewall, the battery, and the truss lattice of the engine mounting system.

Description of work
An inverse design methodology is applied, where an optimization algorithm drives an actual pressure distribution over the intake duct surface towards a desirable target pressure distribution, where the target pressure distribution is expected to bring an improvement to the delivered air quality with acceptable flow characteristics. An aerodynamic functional quantifying the deviation between the actual and

This report is based on a presentation held at the 4th EASN Association International Workshop on Flight Physics and Aircraft Design, Aachen, Germany, October 27-29, 2014.

target pressure distributions is defined, which is to be minimized over the surface of the intake duct. A minimization procedure is performed by means of the NLR's adjoint method ENSENS. The flow simulations are performed using NLR's CFD code ENFLOW.

Results and conclusions

A redesign of the engine intake duct using a CFD-based design optimization method has been performed. The effectiveness of the inverse-by-optimization procedure is demonstrated. To overcome the problem of flow separation in the baseline intake duct, the specification of a target pressure distribution, not necessarily physically realizable, is sufficient to drive the geometry towards one with a desirable pressure gradient. The redesigned engine intake duct demonstrates a principle that a deceleration region should exist, followed by an acceleration region towards the compressor inlet plane inhibiting flow separation.

Applicability

The methodology can be applied to a (re)-design of any duct, in particular when there is a difficulty due to a U- or L-shape of the duct suffering from losses due to flow separation at the corner.

Nationaal Lucht- en Ruimtevaartlaboratorium, National Aerospace Laboratory NLR

Anthony Fokkerweg 2, 1059 CM Amsterdam,
P.O. Box 90502, 1006 BM Amsterdam, The Netherlands
Telephone +31 88 511 31 13, Fax +31 88 511 32 10, www.nlr.nl

Nationaal Lucht- en Ruimtevaartlaboratorium
National Aerospace Laboratory NLR

NLR-TP-2014-528

Aerodynamic design of engine intake duct shape of a general aviation turboprop aircraft

B.I. Soemarwoto, O.J. Boelens and A. Kanakis

This report is based on a presentation held at the 4th EASN Association International Workshop on Flight Physics and Aircraft Design, Aachen, Germany, October 27-29, 2014.

Customer	National Aerospace Laboratory NLR
Contract number	2040207.6.2
Owner	NLR + partner(s)
Division NLR	Aerospace Vehicles
Distribution	Unlimited
Classification of title	Unclassified
	July 2016

Approved by:

Author	Reviewer	Managing department
B.I. Soemarwoto	B.B. Prananta	C.E.J. Wijnberg
Date: 11-12-2017	Date:	Date: 14-12-17

Summary

The aerodynamic design of an engine intake duct shape is described. The design is aimed at obtaining desirable air characteristics into the compressor of a single-engine general aviation turboprop aircraft. The desirable characteristics are based on certain requirements that need to be satisfied for an acceptable quality of the delivered air at a given target mass flow, subject to structural constraints requiring that the shape modification must respect the internal contents of the engine nacelle, such as the firewall, the battery, and the truss lattice of the engine mounting system.

An inverse design methodology is applied, where an optimization algorithm drives an actual pressure distribution over the intake duct surface towards a desirable target pressure distribution, where the target pressure distribution is expected to bring improvement to the delivered air quality with acceptable flow characteristics. An aerodynamic functional quantifying the deviation between the actual and target pressure distributions is defined, which is to be minimized over the surface of the intake duct. A minimization procedure is performed by means of the NLR's adjoint method ENSENS.

The flow simulations are performed using NLR's CFD code ENFLOW. The optimization results show the necessity for a shape modification along the intake duct, implying a flow deceleration in an expanding cross section followed by acceleration in a contracting cross section towards the compressor inlet plane.

Contents

Abbreviations and symbols

AIP	Aerodynamic interface plane
CFD	Computational Fluid Dynamics
DC	Distortion coefficient
EARSM	Explicit Algebraic Reynolds Stress turbulence Model
NLR	Nationaal Lucht- en Ruimtevaartlaboratorium
RANS	Reynolds-Averaged Navier-Stokes
C_L	Lift coefficient
C_D	Drag coefficient
C_M	Pitching moment coefficient
C_p	Pressure coefficient
C_p^*	Target pressure coefficient
p_t	Total pressure
Δp_t	Local deviation of the total pressure
Q	Conservative flow variables
λ	Adjoint variables
θ	Geometric parameters

1 Introduction

One route to deal with aerodynamic design problems is through applying optimisation methodology. In this context, an optimisation problem is defined in terms of aerodynamic objectives to be minimized and constraints to be satisfied. The design variables are the parameters defining the aerodynamic shape. An effective method to solve an optimisation problem is to apply a gradient-based optimisation algorithm. A difficult task in adopting this algorithm is to calculate the gradient efficiently. A well-known brute-force method for computing the gradient is based on finite differencing. This technique is easy to implement but incurs high computational costs, which become prohibitive for a large number of design variables.

An efficient way of computing the gradient for aerodynamic optimisation is to apply the adjoint method, where the effort is independent of the number of design variables. A pioneering work in the application of the adjoint method in fluid dynamics is presented by Pironneau [1] in 1972. However, not before the end of the eighties the potential of the adjoint method for solving industrial design problems was revealed by Jameson [2]. Since then, the adjoint method has captured major industrial, e.g. [3-6], and research interests, e.g. [7-10].

Two routes can be identified in the aerodynamic design methodology:

- *Direct optimization methods*, where the objective and constraints directly define aerodynamic forces and moment coefficients, e.g. C_L, C_D, and C_M. For example, an optimization aimed at drag reduction would be formulated as a minimization problem of C_D for a fixed C_L.
- *Inverse by optimization methods*, where the objective is a functional representing the deviation between an actual pressure distribution and a preferred (target) pressure distribution. Minimization of such a functional, e.g. formulated in a least square sense of $\|p - p_t\|^2$, will lead to a geometry that produces as closely as possible the target pressure distribution.

The second route is taken in this paper. First, a baseline shape of the engine intake duct is analysed by means of a CFD simulation. The resulting flow solution is examined against certain requirements regarding uniformity of the flow. The baseline shape was found to be unsatisfactory because there is a flow separation at the inlet plane towards the compressor. A target pressure distribution along the intake duct is then prescribed with the aim to drive the actual pressure distribution towards a more favourable one through an inverse by optimization procedure, which will result in an improved flow characteristics delivered into the compressor.

The aircraft configuration, procedure and results will be explained in the subsequent sections, covering a description of the CFD and adjoint method used and a comparison between the baseline and optimized intake duct geometry.

2 Aircraft configuration and CFD setup

The aircraft configuration consists of a fuselage, nacelle, spinner, an actuator disk representing the propeller and an engine intake duct. The wing and the tail planes are excluded from the modeling because these components are considered not relevant for the flow inside the intake duct. Figure 1a presents an illustration of the geometry. It should be observed that the detailed compressor geometry is not included. Instead, it is replaced by a tube of a constant diameter having a function as a buffer zone towards the outflow. This buffer zone is indicated as dummy block in Figure 1b, while the inlet plane towards the compressor is designated as the Aerodynamic Interface Plane (AIP).

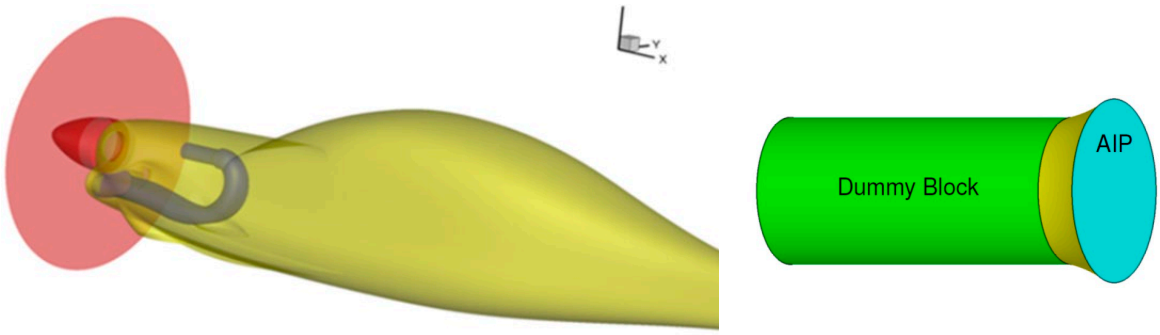

Figure 1 Aircraft configuration and inlet plane definition towards the compressor

The flow simulations are conducted using ENFLOW, a Computational Fluid Dynamics code developed in-house at NLR. The Reynolds-Averaged Navier-Stokes (RANS) equations are applied as the governing equations. Turbulence is incorporated by means of the EARSM k-ω turbulence model [11-13], fully resolving the turbulent boundary layer on the solid wall. The flow domain is represented by a multi-block domain containing structured grids. An impression of the surface grid on the aircraft configuration in the neighborhood of the nacelle is presented in Figure 2a. The grid contains a detailed representation of the geometry around the spinner and the inflow towards the engine intake duct. The volume grid contains a total of about 46.3 million grid cells, from which about 2.5 million grid cells contained inside the intake duct shown Figure 2b.

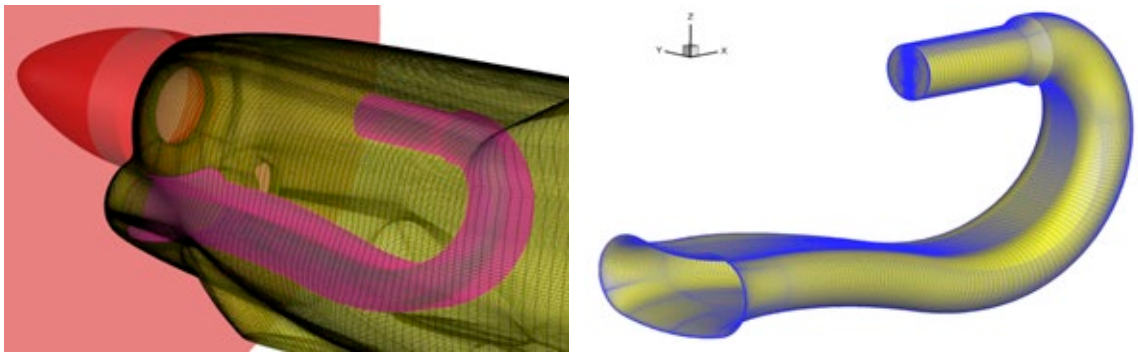

(a) (b)

Figure 2 Illustration of the surface grid on the aircraft and intake duct surface

The design point concerns a subsonic Mach number typical for a general aviation aircraft with the Reynolds number equal to 4 million based on the wing mean aerodynamic chord. The propeller is modelled by means of an actuator disk, where the thrust and power are represented by a uniform distribution of the thrust and tangential force coefficients on the actuator disk. The boundary layer on the whole solid surface are assumed to be turbulent. A back pressure is specified as the boundary condition on the outflow plane from the buffer zone. This back pressure is adjusted during the simulation to give the design mass flow of 1.5 kg/s. A CFD simulation for the design point takes 3 hours on 96 computing cores with convergence accelerations techniques such as multigrid and residual averaging. Figure 3 shows the resulting pressure distribution over all the solid surfaces.

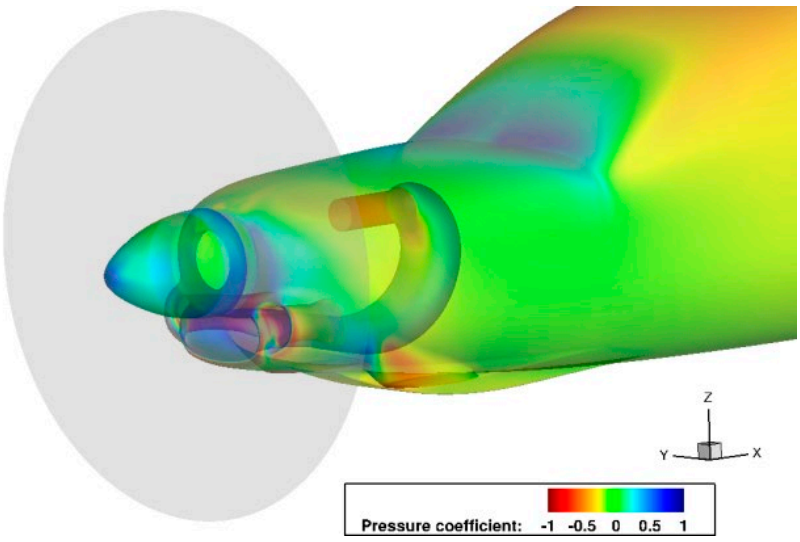

Figure 3 Surface pressure distribution over the aircraft configuration

3 Evaluation of the baseline intake duct

The design requirements for the intake duct are specified as follows:

1. The intake duct must be physically manufacturable, taking into account the material thickness and the airframe dimensional and shaping limitations.
2. The intake duct must be designed to ensure a steady air mass flow rate of 1.5 kg/s.
3. The intake duct must ensure a steady air delivery at the AIP into the compressor with sufficient quality expressed in terms of
   (i) distortion coefficient (DC) which has to be lower than 0.06,
   (ii) local deviation of the total pressure (Δp_t) which has to be between -0.4 and 0.20,
   (iii) total pressure loss along the duct which has to be lower than 0.3.
4. The intake duct must be designed with gradual curves and smooth internal shaping as much as possible.
5. The intake duct must be able to accommodate internal contents of the nacelle, the engine with necessary equipment, the firewall, the battery and the engine mounting system.

Figure 4a shows the total pressure distribution on the AIP. In terms of the above criteria at the AIP, the baseline intake duct violates some of the criteria : (i) upper limit of the distortion coefficient (DC = 0.17), and (ii) lower limit of the total local pressure deviation, ($\Delta p_t = -1.04$). Additionally, a drop in the total pressure at the bottom of AIP is observed, indicating a flow separation, which is confirmed by the limiting streamlines shown in Figure 4b.

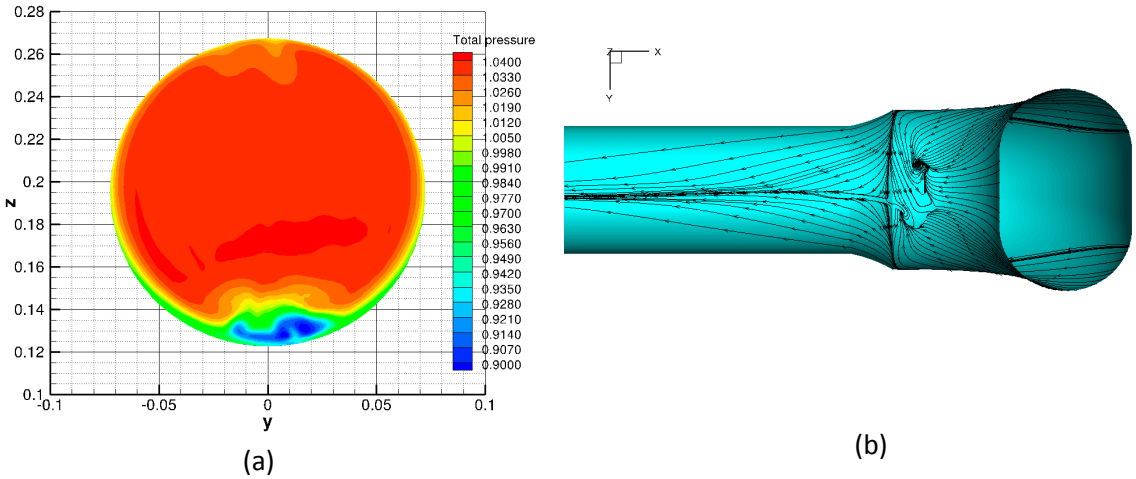

Figure 4 Total pressure contours at the AIP (left) and limiting streamlines on the duct surface (right)

4 Design method

A parametric arc length t is defined along the streamwise direction of the duct, where $t = 0$ and $t = 1$ correspond to the inflow plane into the duct and the AIP, respectively. Circumferentially, another parametric arc length s, $0 \leq s \leq 1$ is defined as shown in Figure 5.

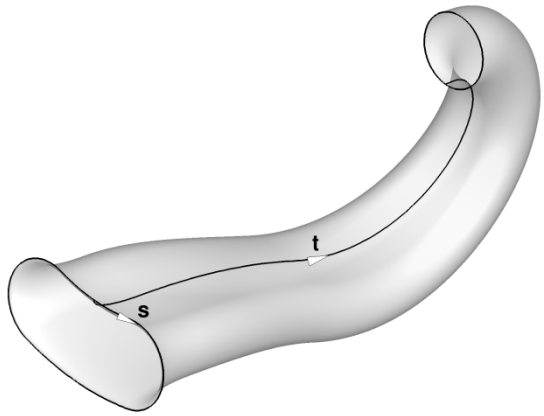

Figure 5 Definition of the parametric arc length s, t

In order to examine the pressure gradient upstream of the AIP, an inviscid flow simulation based on the Euler equations is performed for the isolated intake duct. The boundary conditions at the inflow and outflow of the isolated intake duct are obtained from the previous viscous (RANS) simulation around the complete aircraft configuration. This determines the distribution of the total pressure, total temperature and velocity vector at the inflow, and the back pressure at the outflow. Figure 6a shows the inviscid pressure distribution along $0 \leq t \leq 1$ at $s = 0, 0.25, 0.5, 0.75$.

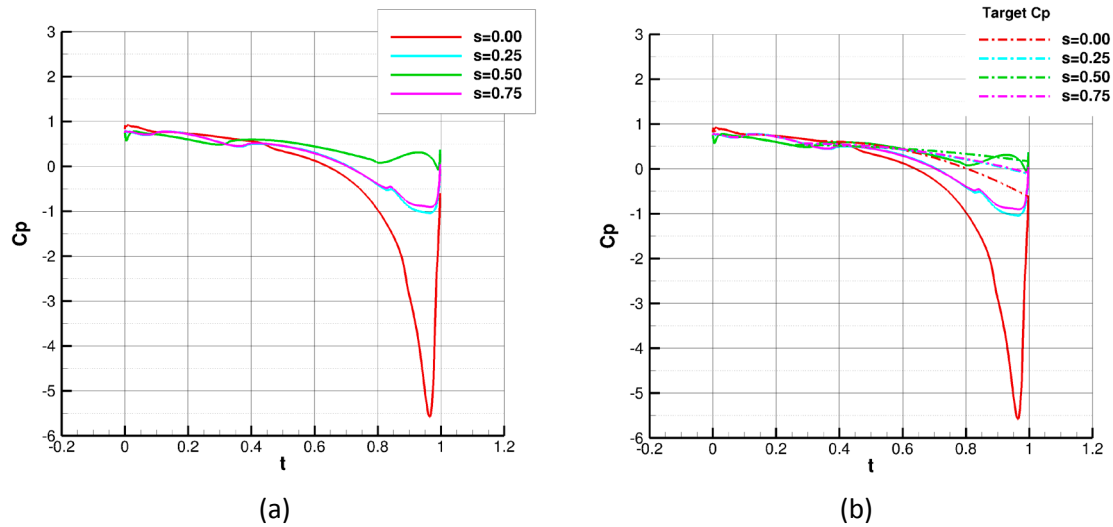

(a) (b)

Figure 6 Baseline inviscid pressure distribution and target pressure distribution

The pattern of the total pressure and the flow separation shown in Figure 4 can be attributed to the adverse inviscid pressure gradient occurring in the regions of $t \geq 0.96$. One way to eliminate the flow separation is to modify the geometry through an inverse method, such that it will achieve a specified target pressure distribution having a desirable gradient. However, specifying a three dimensional target pressure distribution is a formidable task, more so if it were to be physically realizable. A more practical approach taken in the present study is to specify a target pressure distribution which does not necessarily have to be physically realizable, but with the intention only to drive the current pressure distribution towards a more desirable one. This is to be achieved by minimizing a functional I defined over the surface S of the form

$$I = \int \left(C_p - C_p^*\right)^2 dS \tag{1}$$

where C_p^* is the target pressure distribution. This target pressure distribution is shown in Figure 6b at four values of s, where for the location in between them a cubic spline interpolation is applied. The minimization is carried out using the adjoint method based on the inviscid Euler equations as follows. Assuming adiabatic flow and no external body force, the conservation law for steady inviscid flows can be written in the divergence form as

$$\nabla . F(Q) = 0 \tag{2}$$

in a flow domain Ω bounded by the surface S having a shape defined by a vector of geometric parameters θ. In this case, θ determines the shape of the intake duct. $F(Q)$ is the flux vector which is a function of the flow variables Q defining air density, velocity and pressure. The solution of the flow equation (2), subject to a solid-wall boundary condition, provides the values of the flow variables Q. For the Euler equations, the slip solid-wall boundary condition is applied which can be expressed as:

$$B(Q, \theta) = 0 \tag{3}$$

A Lagrangian L is introduced by augmenting the functional (1) with the flow equation (2) and the solid-wall boundary condition (3) by means of Lagrange multipliers λ and γ:

$$L = \int \left(C_p - C_p^*\right)^2 dS + \int \lambda \nabla . F(Q)\, d\Omega + \int \gamma B(Q, \theta)\, dS \tag{4}$$

where λ is referred to as the adjoint variables, the elements of which correspond to the elements of the flow variables Q. The variation of the Lagrangian is due to the independent variations of the adjoint variables, flow variables, Lagrange multipliers and geometric parameters:

$$\delta L = \delta L_\lambda + \delta L_\gamma + \delta L_Q + \delta L_\theta \tag{5}$$

where the notation δL_λ refers to the variation of L due to the variation of λ. It can easily be verified that the terms δL_λ and δL_γ vanish as the flow equation (2) and the boundary condition (3) are satisfied, such that

$$\delta L = \delta L_Q + \delta L_\theta \tag{6}$$

Setting δL_Q to zero leads to a set of conditions which are referred to as the adjoint equations and boundary conditions. Satisfying these conditions implies $\delta L = \delta L_\theta$, or equivalently $\delta L = L_\theta\ \delta\theta$, where L_θ is equivalent with the gradient of the functional I with respect to the geometric parameters θ. This gradient is used by an optimization algorithm to minimize the functional I. Figure 7a shows the optimization history where the functional has reduced by two orders of magnitude. Figure 7b shows the final pressure distribution, which should be compared with that in Figure 6, demonstrating that the adverse pressure gradient has been eliminated, or mitigated enormously at $s = 0$.

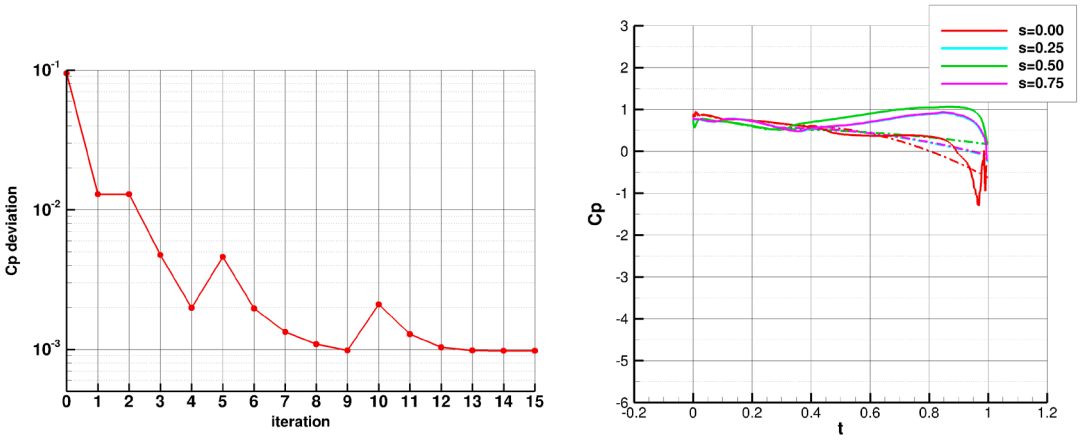

(a) (b)

Figure 7 Optimization history and optimized inviscid pressure distribution

5 Evaluation of the redesigned intake duct

The intake duct optimized by means of the inverse method described above is placed back to the complete aircraft configuration depicted in Figure 1. Subsequently, another viscous flow simulation using the RANS equations is performed. Figure 8a presents a comparison of the total pressure loss on the symmetry plane of the duct. Although the difference seems to be small, the flow separation at the AIP has been eliminated. Figure 8b presents the pattern of the term that determines the distortion coefficient. It is clear that the flow separation occuring in the baseline intake duct is the culprit. The redesign has improved the distortion coefficient on the AIP from DC = 0.17 to DC = 0.034, now well below the upper limit of 0.06.

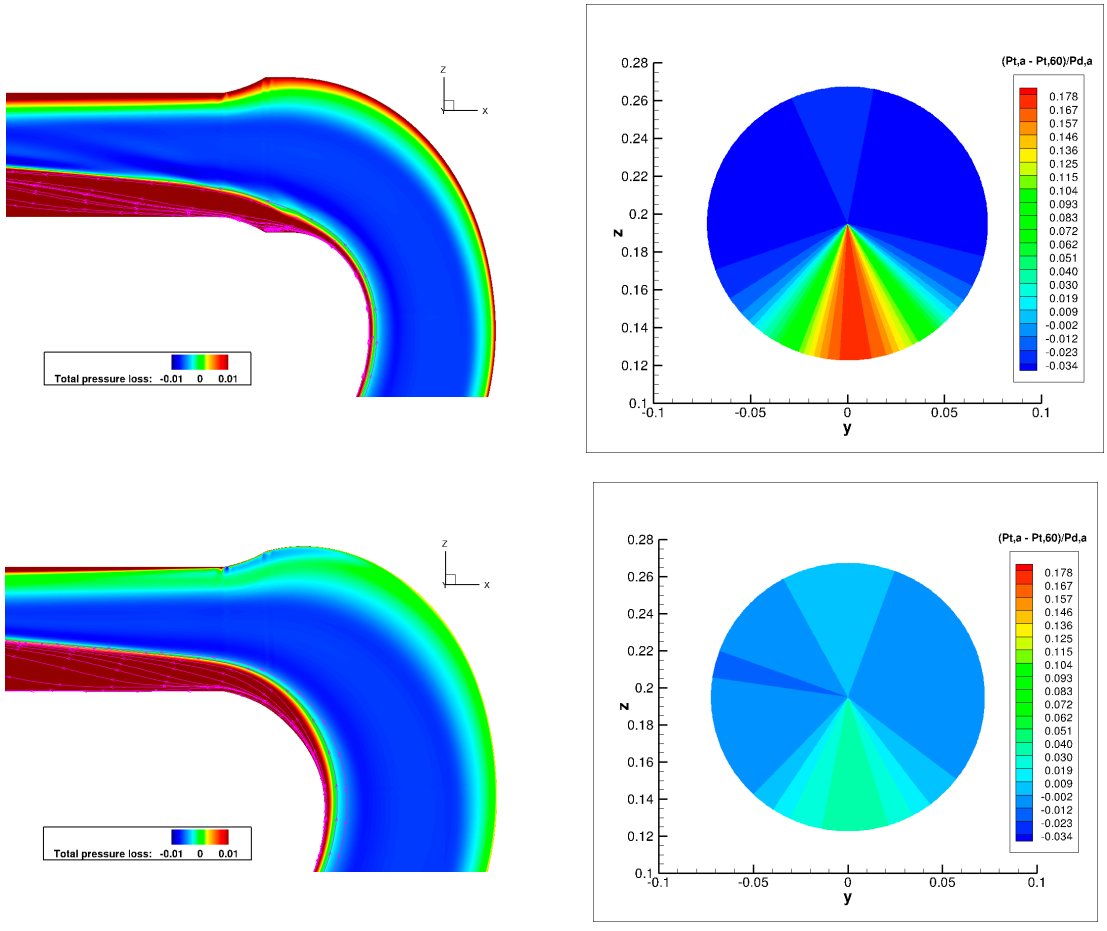

(a) Streamline pattern

(b) distortion coefficient

Figure 8 Comparison between the baseline (upper) and optimized (lower) intake duct

The impact of the design can also be clearly seen in Figure 9a in terms of the local deviation of the total pressure. The minimum value has been improved from -1.03 to -0.93. It is indeed still far away from the lower limit of -0.4. However, one should also observe where this limit is violated. Figure 9b presents the contours of the local deviation with values above -0.4 blanked, in order to show the region where the criterion is violated. It shows that in the baseline intake duct this region will impinge on the compressor blade. On the other hand, in the optimized intake duct, this region is located well inside the boundary layer, most probably within the tip clearance of the compressor blade.

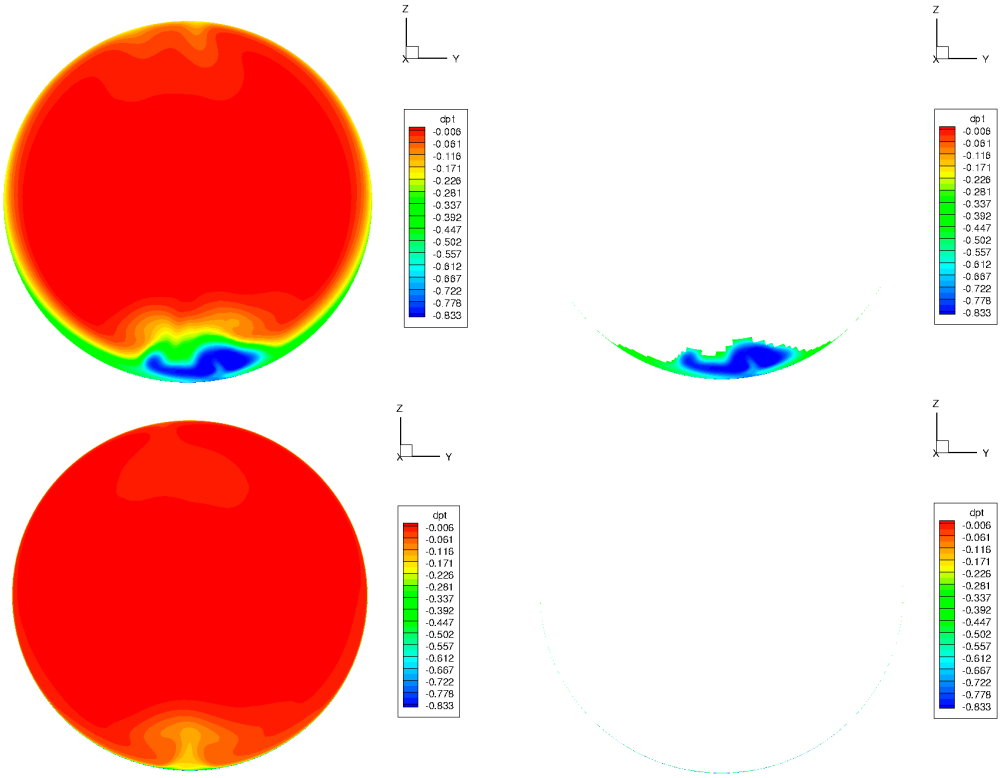

(a) total pressure deviation (b) total pressure deviation ≤ -0.4

Figure 9 Comparison between the baseline (upper) and optimized (lower) intake duct

Figure 10 gives an impression of the impact of the design to the geometry of the intake duct. The necessity for a change to a larger cross section of the duct towards the diameter of the AIP is a logical consequence. It shows the necessity for a shape modification along the intake duct, implying a flow deceleration in an expanding cross section followed by acceleration in a contracting cross section towards the compressor inlet plane, resulting in a favourable pressure gradient inhibiting flow separation.The pattern of the surface limiting streamlines shown in in the figure on the right confirms that there is no flow separation along the optimized intake duct.

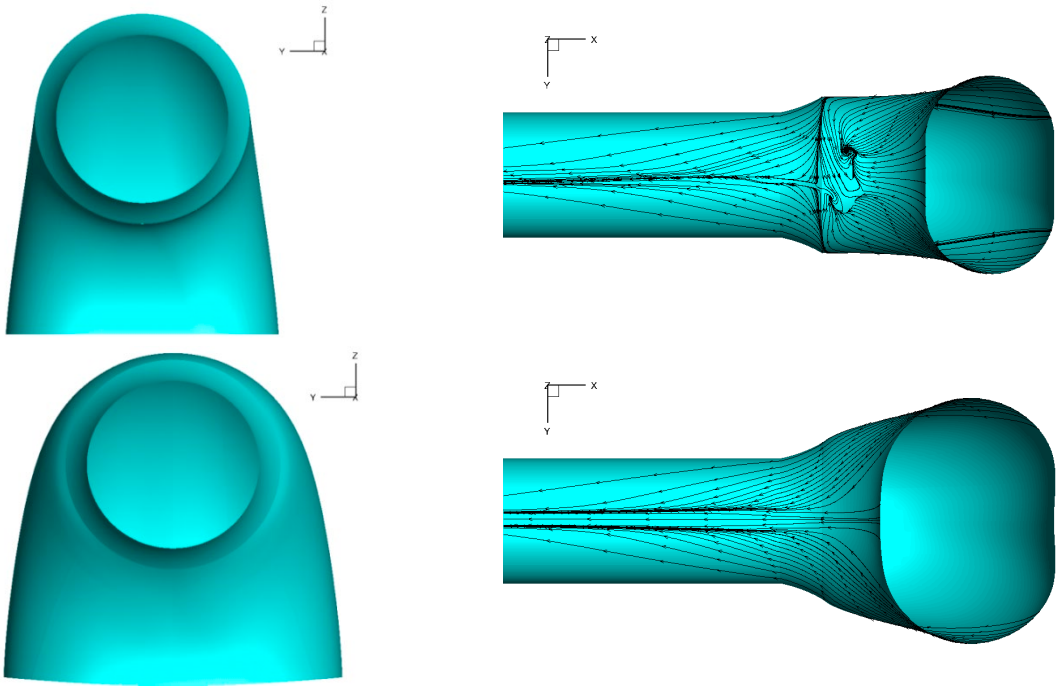

Figure 10 Comparison between the baseline (upper) and optimized (lower) intake duct

6 Conclusions

A redesign of the engine intake duct using a CFD-based design optimization method has been performed. The method employs the adjoint method which is applied to an inverse procedure minimizing the deviation between the actual pressure distribution and a desirable target pressure distribution. The effectiveness of the inverse procedure has been demonstrated. To overcome the problem of flow separation in the baseline intake duct, the specification of a physically unrealizable target pressure distribution is sufficient to drive the geometry towards one with a desirable pressure gradient. The redesigned engine intake duct features a deceleration region followed by an acceleration region inhibiting flow separation towards the compressor inlet plane.

Acknowledgment

The paper was prepared in the frame of the research project: ESPOSA (Efficient Systems and Propulsion for Small Aircraft) partly funded under 7th FP of the EU, Grant Agreement No. ACP1-GA-2011-284859-ESPOSA.

References

[1] O. Pironneau. On optimum profile in stokes flow. Journal of Fluid Mechanics, (59):117–128, 1972.

[2] Jameson. Aerodynamic design via control theory. Journal of Scientific Computing, Vol. 3, No. 3, 1988.

[3] Jameson. Re-Engineering the Design Process Through Computation. Journal of Aircraft, Vol. 36, No. 1, January-February 1999.

[4] J.C. Vassberg and A. Jameson. Aerodynamic shape optimization of a Reno race plane. Intl. J. Vehicle Design, Vol. 28, No. 4, pp. 318-338, 2002.

[5] B.I. Soemarwoto, M. Laban, A. Jameson, A.L. Martins and B. Oskam. Adaptive Aerodynamic Optimization of Regional Jet Aircraft, AIAA 2002-0260, 40th AIAA Aerospace Sciences Meeting and Exhibit, January 14–17, 2002/Reno, NV.

[6] M. Laban, B.I. Soemarwoto and J.W. Kooi. Reshaping Engine Nacelles for Testing in Wind Tunnels with Turbofan Propulsion Simulators, AIAA-2005-3703, 41st AIAA/ASME/SAE/ASEE Joint Propulsion Conference & Exhibit, 10 - 13 July 2005, Tucson, Arizona.

[7] S.K. Nadarajah and A. Jameson. Studies of the continuous and discrete adjoint approaches to viscous automatic aerodynamic shape optimization. AIAA-2001-2530, 2001.

[8] E. J. Nielsen and W. Kyle Anderson. Recent Improvements in Aerodynamic Design Optimization on Unstructured Meshes. AIAA Journal, Vol. 40, No. 6, June 2002.

[9] D.I. Papadimitriou, K.C. Giannakoglou, The Continuous Direct-Adjoint Approach for Second Order Sensitivities in Viscous Aerodynamic Inverse Design Problems, Computers & Fluids, 38, pp. 1539-1548, 2009.

[10] Z.Lyu, G.K.W. Kenway, J.R.R.A. Martins, RANS-based Aerodynamic Shape Optimization Investigations of the Common Research Model Wing, AIAA Paper 2014-0567.

[11] J.C. Kok, J.W. Boerstoel, A. Kassies, and S.P. Spekreijse, A Robust Multi-Block Navier-Stokes Flow Solver for Industrial Applications, Proceedings of ECCOMAS Conference, Paris, 1996, also NLR-TP-96323, 1996.

[12] J.C. Kok, Resolving the dependence on freestream values for the k-ω turbulence model, AIAA Journal, 38(7), pp. 1292–1294, 2000.

[13] H.S. Dol, J.C. Kok, and B. Oskam, Turbulence Modelling for Leading-Edge Vortex Flows, AIAA-2002-0843, January 2002.